The Influence of Changes in Cloud Cover on Recent Surface Temperature Trends in the Arctic

YINGHUI LIU

Cooperative Institute for Meteorological Satellite Studies, University of Wisconsin—Madison, Madison, Wisconsin

JEFFREY R. KEY

Office of Research and Applications, NOAA/NESDIS, Madison, Wisconsin

XUANJI WANG

Cooperative Institute for Meteorological Satellite Studies, University of Wisconsin—Madison, Madison, Wisconsin

(Manuscript received 15 September 2006, in final form 29 May 2007)

ABSTRACT

A method is presented to assess the influence of changes in Arctic cloud cover on the surface temperature trend, allowing for a more robust diagnosis of causes for surface warming or cooling. Seasonal trends in satellite-derived Arctic surface temperature under clear-, cloudy-, and all-sky conditions are examined for the period 1982–2004. The satellite-derived trends are in good agreement with trends in the European Centre for Medium-Range Weather Forecasts (ECMWF) reanalysis product and surface-based weather station measurements in the Arctic. Surface temperature trends under clear and cloudy conditions have patterns similar to the all-sky trends, though the magnitude of the trends under cloudy conditions is smaller than those under clear-sky conditions, illustrating the negative feedback of clouds on the surface temperature trends. The all-sky surface temperature trend is divided into two parts: the first part is a linear combination of the surface temperature trends under clear and cloudy conditions; the second part is caused by changes in cloud cover as a function of the clear–cloudy surface temperature difference. The relative importance of these two components is different in the four seasons, with the first part more important in spring, summer, and autumn, but with both parts being equally important in winter. The contribution of biases in satellite retrievals is also evaluated.

1. Introduction

A variety of recent studies have shown that the Arctic is expected to warm more than any other part of the earth in response to increasing concentrations of greenhouse gases, largely because of polar amplification due to feedback effects associated with the high albedo of snow and ice (cf. Manabe et al. 1992). Arctic surface temperatures are projected to rise at a rate about twice the global mean over the next century (Houghton et al. 2001). Surface temperature is an extremely important climate change variable, because it integrates changes in the surface energy budget and atmospheric circulation (Serreze et al. 2000).

Due to the paucity of conventional observations in the Arctic, especially over the Arctic Ocean, an evaluation of trends in surface temperature is challenging. Rigor et al. (2000) analyzed the seasonal mean and trends of surface air temperature based on observations from buoys, manned drifting stations, and land meteorological stations, with interpolation to fill gaps, in the Arctic from 1979 to 1997. The dataset is a part of the International Arctic Buoy Program/Polar Exchange at the Sea Surface (IABP/POLES). The limitations of their work include the relatively small amount of observations over the Arctic Ocean and the poor quality of the buoy data, especially before 1992. Satellite data provide an opportunity to investigate the surface temperature over the entire Arctic region by its high tem-

Corresponding author address: Yinghui Liu, Cooperative Institute for Meteorological Satellite Studies, University of Wisconsin—Madison, 1225 West Dayton Street, Madison, WI 53706.
E-mail: yinghuil@ssec.wisc.edu

DOI: 10.1175/2007JCLI1681.1

poral and spatial resolution cover over high latitudes. Chen et al. (2002) derived surface temperatures from the Television and Infrared Observation Satellite Operational Vertical Sounder Polar Pathfinder (TOVS Path-P) dataset and compared the decadal temperature trends calculated from TOVS and the POLES dataset. They found large discrepancies in the decadal temperature trends over the central Arctic Ocean in spring. Comiso (2003) studied the seasonal trend of surface temperature during cloud-free conditions based on satellite thermal infrared data from the Advanced Very High Resolution Radiometer (AVHRR), a five-channel imager on board the National Oceanic and Atmospheric Administration (NOAA) polar orbiting satellites. He found that the trends in cloud-free surface temperature are mainly positive in summer, spring, and autumn; the trends are generally negative in winter, with some cooling observed in large areas in the Bering Sea and parts of Russia. Wang and Key (2003, 2005a,b) investigated recent trends in Arctic surface, cloud, and radiation properties in the Arctic from 1982 to 1999 based on the extended AVHRR Polar Pathfinder (APP-x) product. For the all-sky (clear and cloudy) surface temperature, they found a cooling trend in winter over the central and eastern Arctic Ocean and mainly warming trends in spring, summer, and autumn. Over the central and eastern Arctic Ocean there was also a significant decreasing trend in cloud cover in winter.

Changes of surface temperature are related to changes of large-scale atmospheric circulation. The Arctic Oscillation (AO; Thompson and Wallace 1998) is the principal component of the Northern Hemisphere sea level pressure poleward of 20°N. Using an East Anglian surface air temperature dataset, Thompson et al. (2000) showed that the AO accounts for as much as 50% of the winter (November–April) warming over the Eurasia land areas due to warm air advection. Rigor et al. (2000) showed that the AO accounts for 74% of the warming over the eastern Arctic Ocean and 14% of the cooling over the western Arctic during the winter from 1979 to 1997.

Changes of surface temperature are also related to the changes in sea ice cover. Parkinson et al. (1999) reported that the total Arctic sea ice extent decreased by approximately 34 300 km^2 yr^{-1} from 1978 to 1996, Parkinson and Cavalieri (2002) showed the decreasing rate of ice extent of about 32 900 km^2 yr^{-1} from 1979 to 1999, and Cavalieri et al. (2003) showed a decreasing rate of ice extent of about 36 000 km^2 yr^{-1} for 1979–2002. Liu et al. (2004) showed pronounced decreases of satellite-derived Arctic sea ice concentrations in the Barents–Kara Seas, between the Chukchi and Beaufort Seas, the central Sea of Okhotsk, and a portion of the Hudson–Baffin Bay. Rigor et al. (2002) argued that increased advection of ice away from the coast, and a cyclonic sea ice motion anomaly in winter during high index conditions of the AO, contributed to the thinning of sea ice, which contributed to the observed trends in sea ice concentration, extent, and thickness, and to the observed trends in surface temperature both in winter and in the ensuing seasons.

To understand the Arctic climate system we must understand cloud processes, including their interaction with atmospheric dynamics and their influence on the surface (Curry et al. 1996). Clouds have a strong radiative influence on the energy budget both at the surface and top of the atmosphere (Dong and Mace 2003; Intrieri et al. 2002; Shupe and Intrieri 2004). Their impact on radiation fluxes depends on cloud amount, phase, particle size, and their vertical and horizontal distributions (Randall et al. 1998; King et al. 2004). Clouds act to warm the Arctic surface for most of the annual cycle with a brief period of cooling in the middle of summer (Intrieri et al. 2002; Curry and Ebert 1992; Walsh and Chapman 1998; Key et al. 1999; Shupe and Intrieri 2004). Polar cloudiness is expected to change considerably if decreasing sea ice cover creates larger areas of open water and the varying atmospheric circulation changes the moisture advection into Arctic (Walsh and Chapman 1998; Groves and Francis 2002). Trends in satellite-derived clouds show that the Arctic has become cloudier in spring and summer but becomes less cloudy in winter (Wang and Key 2003, 2005b).

There are significant surface temperature differences under cloudy and clear conditions, with an observed difference of 8–10 K during October–February and 5–6 K during March–May and September (Walsh and Chapman 1998). Given significant surface temperature differences under cloudy and clear conditions, trends in cloud amount can have a profound influence on a trend of surface temperature. In this study, satellite-derived Arctic surface temperature trends under cloudy-, clear-, and all-sky conditions and their differences are presented. A method is presented to investigate and quantify the influence of changes in Arctic cloud cover on the surface temperature trend, which is the focus of this study.

2. Data and analysis methods

The APP-x dataset extends the APP (see nsidc.org/data/docs/daac/nsidc0066_avhrr_5km.gd.html and Meier et al. 1997) products to include cloud optical depth, cloud particle phase and size, cloud-top tem-

perature and pressure, all-sky surface temperature and broadband albedo, and radiative fluxes. Retrievals were done with the Cloud and Surface Parameter Retrieval system (CASPR; Key 2002; Key et al. 2001; Key and Intrieri 2000), which was specifically designed for polar AVHRR daytime and nighttime data. Cloud detection is done with a variety of spectral and temporal tests optimized for high-latitude conditions (Key and Barry 1989). The clear-sky surface skin temperature is retrieved using a split-window technique (Key and Haefliger 1992; Key et al. 1997). A regression model was developed to estimate the cloudy-sky surface temperature from nearby clear-sky temperatures, wind speed, and solar zenith angle (day time) (Key and Wong 1999; Key 2002). In terms of the annual cycle of the total cloud fraction, the APP-x dataset provides a reliable estimate of cloud fraction when compared to surface observations (Wang and Key 2005a). The APP-x parameters have been validated with data collected during the Surface Heat Budget of the Arctic Ocean (SHEBA; Uttal et al. 2002) field experiment in the western Arctic (Key et al. 2001; Maslanik et al. 2001; Stroeve et al. 2001; Key and Intrieri 2000; Wang and Key 2003), and results show reasonable agreement between APP-x retrieved cloud microphysical properties and in situ observations. Comparisons between APP-x and SHEBA ship measurements show a 0.2-K bias and a 1.98-K root-mean-square (RMS) error in the surface skin temperature under clear conditions (Wang and Key 2005a) and a −1.6-K bias and 6-K RMS error under all-sky conditions. An examination of the intercalibration between satellites reveals no observable bias or inconsistency. A comparison of the APP-x all-sky temperature to the surface air temperature measurements from 41 Arctic meteorological stations shows that the two surface temperature datasets are consistently within 1 to 3 K of each other throughout the 1982 to 1999 period, and that the trends are similar in magnitude and sign (Wang and Key 2003). Additional details on the validations can be found in the supporting materials of Wang and Key (2003).

The APP-x dataset includes daily composites at both 0400 and 1400 local solar standard time (LST) from January 1982 to December 2004 at a 25-km spatial resolution (5-km pixels sampled every 25 km). Monthly means of cloud cover and surface temperature under cloud-free and cloudy- and all-sky conditions are calculated from the twice-daily data. At least 10 daily values in a month are required in the calculation of the monthly means. Due to the extensive cloudiness of the Arctic, daily cloud-free and cloudy data are remapped to a 100-km grid by averaging. The seasonal means are calculated based on the monthly means in winter (December–February), spring (March–May), summer (June–August), and autumn (September–November). In this paper, only the results at 1400 LST are presented and analyzed, but conclusions based on both times are similar.

The 40-yr European Centre for Medium-Range Weather Forecasts (ECMWF) Re-Analysis (ERA-40) products (Uppala et al. 2005) are also used in this study. Most of the ERA-40 archived output is available 4 times daily at a resolution of 2.5° latitude by 2.5° longitude from September 1957 to August 2002. In this paper, the monthly mean surface air temperature, which is the monthly mean of all four daily times, from January 1982 to August 2002, is employed. The seasonal mean is calculated based on the monthly mean data. The seasonal trends of each parameter are derived based on the seasonal means. Trend analysis was performed using the least squares fit regression, where the trend value is the slope of the regression line. For each trend, an *F*-test value of significance is computed.

3. Surface temperature trends

The seasonal trends of all-sky surface temperature based on APP-x dataset from 1982 to 2004 are calculated on a pixel-by-pixel basis and the results are presented in Fig. 1a. In winter, the surface temperature increases over northern Canada, with the maximum magnitude over Hudson Bay. The surface temperature decreases over the Arctic Ocean and the eastern Arctic. Over the central Arctic Ocean, the decreasing trend is approximately −2.5 K decade^{-1}. This cooling trend is consistent with the positive sea ice extent trend over the Arctic Ocean and Bering Sea in the same season (Parkinson et al. 1999). In spring, significant warming is seen over most of the Arctic, including the central Arctic Ocean, most of northern Canada and Alaska, and north-central Russia. The maximum increasing trend is around 2.0 K decade^{-1} over land and over the Chukchi and Beaufort Seas. In summer, the surface temperature is generally increasing, with a smaller magnitude than those in spring. The strong increasing trend can be seen over northeastern Russia, Alaska, and northern Canada with the maximum trend around 1.5 K decade^{-1}. Over the central Arctic Ocean and north-central Russia, the trends are near 0. In autumn, there are strong increasing surface temperature trends over Beaufort Sea, Chukchi Sea, Alaska, and northern Canada, with the maximum trend around 2.0 K decade^{-1}. This warming trend is closely related to the sea ice cover retreat in the 1990s (McPhee et al. 1998; Comiso 2001). The trend over most of the Arctic Ocean is negative, with the magnitude around −0.5 K decade^{-1}. In four seasons,

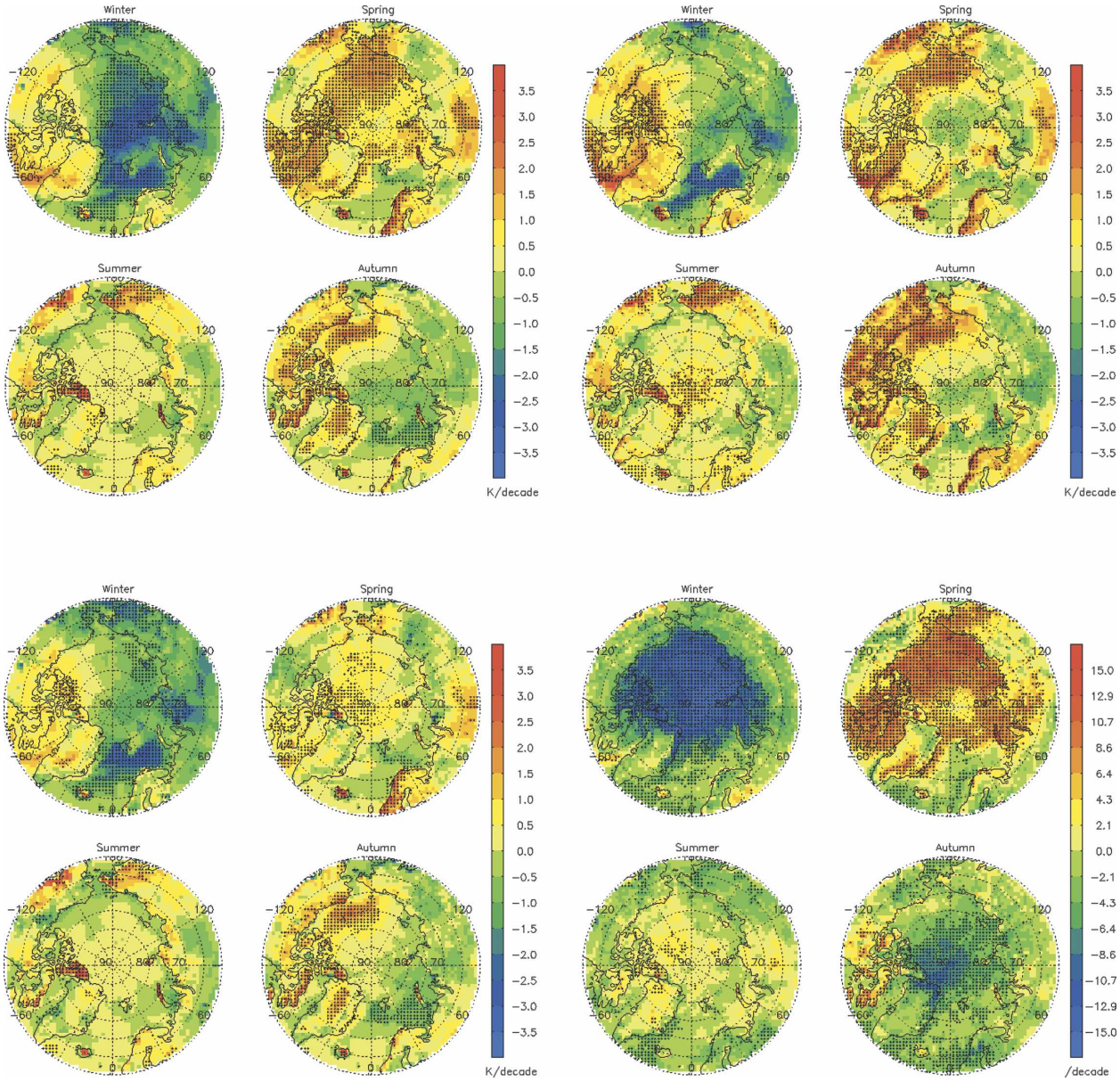

FIG. 1. Seasonal (top left quadrant) all-, (top right) clear-, and (bottom left) cloudy-sky surface temperature trends and (bottom right) cloud cover trends from 1982 to 2004 based on APP-x dataset. A trend with a confidence level larger than 95% based on the *F* test is indicated with a very small plus sign.

the surface temperature trends over northern Europe are positive, with the strongest increasing in spring of 2.0 K decade^{-1}. The trends based on the APP-x all-sky surface temperature at 0400 LST are similar (not shown).

The all-sky surface temperature trends from the APP-x dataset in four seasons are compared with the surface air temperature trends from ERA-40 reanalysis grid point by grid point, after the APP-x trends are sampled to the ERA-40 grid. It should be noted that AVHRR data were not assimilated in the ERA-40 reanalysis. The APP-x trends are calculated based on the APP-x all-sky surface skin temperature at 1400 LST; the ERA-40 trends are calculated based on the monthly mean of all four daily times of surface air temperature. The trends from 1982 to 2001 are calculated instead of 1982 to 2004, as ERA-40 ends at August 2002. Overall there is good agreement between APP-x surface skin temperature trends and ERA-40 surface air temperature trends in four seasons. The average biases between them in winter, spring, summer, and autumn are −0.40, −0.05, 0.13, and −0.31 K decade^{-1}; the RMS differ-

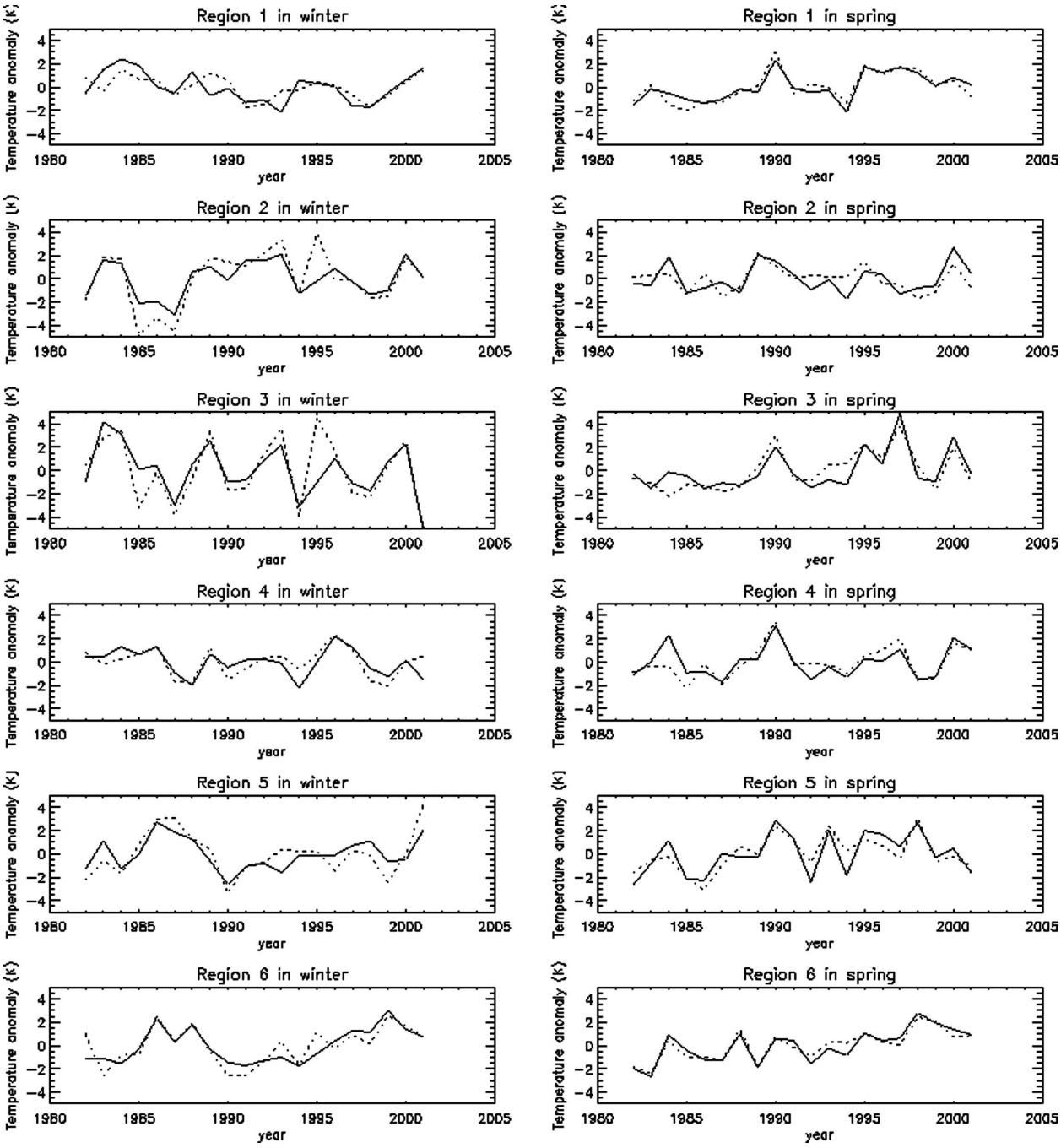

FIG. 2. Time series of regional mean, seasonal APP-x surface skin temperature anomalies (solid lines), and ERA-40 surface air temperature anomalies (dotted lines) in winter and spring for selected regions.

ences are 0.80, 0.63, 0.50, and 0.65 K decade^{-1}; and the correlation coefficients between these two trends in four seasons are 0.60, 0.56, 0.43, and 0.53, respectively. Time series of seasonal anomalies of the APP-x surface skin temperature and the ERA-40 surface air temperature over selected regions are shown in Fig. 2 [region 1: Arctic basin (Groves and Francis 2002); region 2: northern Europe; region 3: north-central Russia; region 4: northeastern Russia; region 5: Alaska; region 6: northern Canada]. Due to a gap in AVHRR data during the 1995 winter, the data are interpolated between the 1994 and 1996 winters. These two anomalies show good agreement. It should be noted that ECMWF reanalysis is not an in situ observation. Further validation of these

two datasets with in situ observations, as done in Wang and Key (2003), is needed.

Surface temperature trends from 1982 to 2004 under cloud-free and cloudy conditions in four seasons based on the APP-x dataset are calculated in the same way as the all-sky trends. They are shown in Figs. 1b and 1c. The cloudy-sky surface temperature trends could be a result of changes in cloud properties, atmospheric circulation and heat advection, and/or sea ice cover. The clear-sky surface temperature trends might result from the changes in the atmospheric circulation, heat advection, and/or sea ice cover. The cloud-free and cloudy surface temperature trends exhibit similar patterns as the all-sky trends shown in Fig. 1a.

The differences in surface temperature trends under clear and cloud conditions are due not only to changes in cloud cover, but also changes in cloud properties. For example, there is a decreasing trend in APP-x cloud-top height (increasing cloud-top pressure) in the Chukchi Sea and central Arctic in winter (Wang and Key 2005a,b). This change might contribute to the stronger cooling trend over the Chukchi Sea and central Arctic in winter under cloudy conditions than under clear conditions, as warmer clouds emit more longwave radiation upward. APP-x shows a decreasing trend in cloud optical depth corresponding to a higher frequency of ice cloud at the North Pole in winter, which results in a negative trend in longwave cloud radiative forcing at the surface under cloudy conditions. This change is consistent with the stronger cooling trend near the pole in winter under cloudy conditions than under clear conditions.

However, for regions where both clear and cloudy trends are positive— including most of North America in winter, the Chukchi and Beaufort Seas in spring, the central Arctic Ocean in summer, and most of North America, the Chukchi and Beaufort Seas in autumn— the magnitude of the warming trends under cloud-free conditions is larger than under cloudy conditions. For the regions where both trends are negative, including the eastern Arctic Ocean and north-central Russia in winter, and part of northeastern Russia in spring, the magnitude of both trends are comparable. Under cloudy conditions, the trends are not as dramatic as under cloud-free conditions, which tend to imply that clouds have a negative feedback on the surface temperature trends, as pointed out by Wang and Key (2003).

4. The influence of clouds on all-sky temperature trends

Over the Arctic, especially over the Arctic Ocean, clouds warm the surface at all times of the year except during a portion of the summer (Curry et al. 1993; Schweiger and Key 1994; Walsh and Chapman 1998; Intrieri et al. 2002). As a result, the difference between the cloudy and the cloud-free seasonal mean surface temperature is 8–10 K during October–February and 5–6 K during March–May and September over sea ice based on in situ observations (Walsh and Chapman 1998). Therefore, if the surface temperature under cloud-free and cloudy conditions remain constant (but different from each other), and cloud cover changes over the years, the all-sky surface temperature observed from satellite will, of course, change.

Can we quantify the influence of cloud cover trends on the all-sky surface temperature trend? To answer that question a linear model is used. The clear and cloudy surface temperature and cloud cover are assumed to change linearly over a time period of Z years, for example, from 1982 to 2004. The surface temperature retrieval with satellite data is assumed to have biases Δ_{clr} for cloud-free and Δ_{cld} for cloudy conditions; these biases do not change over time. At the beginning of the time period, the cloud-free surface temperature is $T_{clr,1} + \Delta_{clr}$, where $T_{clr,1}$ is the unbiased real cloud-free surface temperature. Similarly, the cloudy surface temperature is $T_{cld,1} + \Delta_{cld}$, where $T_{cld,1}$ is the unbiased real cloudy surface temperature; the cloud cover is C_1 All three parameters change linearly with time. At the end of the Z years, the cloud-free surface temperature is $T_{clr,2} + \Delta_{clr}$; the cloudy surface temperature is $T_{cld,2} + \Delta_{cld}$; and the cloud cover is C_2. The trends of the cloud-free surface temperature, cloudy surface temperature, and cloud cover are S_{clr}, S_{cld}, and S_c, respectively. The means of the cloud-free surface temperature, the cloudy surface temperature, and cloud cover over this time period are T_{clr}, T_{cld}, and C, respectively. The relationships between these variables are

$$
\begin{aligned}
T_{clr,2} + \Delta_{clr} &= T_{clr,1} + \Delta_{clr} + S_{clr}Z,\\
T_{cld,2} + \Delta_{cld} &= T_{cld,1} + \Delta_{cld} + S_{cld}Z,\\
C_2 &= C_1 + S_cZ,\\
T_{clr} &= (T_{clr,1} + T_{clr,2})/2 + \Delta_{clr}\\
&= T_{clr,real} + \Delta_{clr},\\
T_{cld} &= (T_{cld,1} + T_{cld,2})/2 + \Delta_{cld}\\
&= T_{cld,real} + \Delta_{cld}, \quad \text{and}\\
C &= (C_1 + C_2)/2,
\end{aligned}
$$

where $T_{clr,real}$ and $T_{cld,real}$ are the real (true) mean of the cloud-free and cloudy surface temperature without retrieval biases. In the following sections, the seasonal means of the cloud-free surface temperature, the cloudy surface temperature, and cloud cover are calcu-

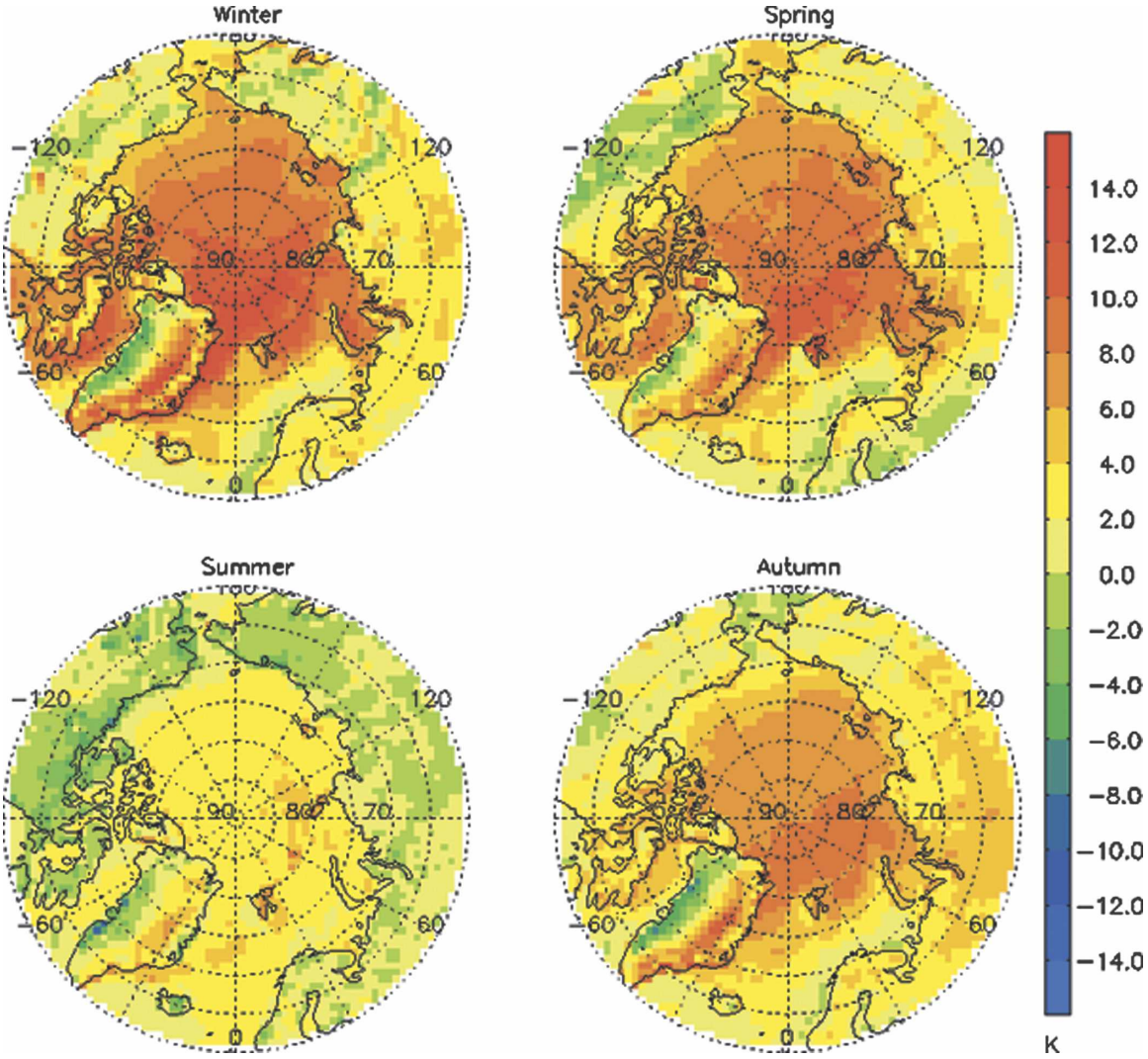

FIG. 3. The difference between the seasonal mean surface temperature (K) under cloudy and cloud-free conditions based on the APP-x dataset.

lated as the means of all the individual seasonal means, not the averages of the seasonal means in the first and last years. Then the all-sky surface temperatures at the beginning and end of the time series and the trend are

$$T_{\mathrm{all},1} = (T_{\mathrm{clr},1} + \Delta_{\mathrm{clr}})(1 - C_1) + (T_{\mathrm{cld},1} + \Delta_{\mathrm{cld}})C_1,$$

$$T_{\mathrm{all},2} = (T_{\mathrm{clr},2} + \Delta_{\mathrm{clr}})(1 - C_2) + (T_{\mathrm{cld},2} + \Delta_{\mathrm{cld}})C_2 S_{\mathrm{all}} = (T_{\mathrm{all},2} - T_{\mathrm{all},1})/Z.$$

It can be shown from the above equations that

$$S_{\mathrm{all}} = [S_{\mathrm{clr}}(1 - C) + S_{\mathrm{cld}}C] + (T_{\mathrm{cld}} - T_{\mathrm{clr}})S_c, \quad (1)$$

$$S_{\mathrm{all}} = [S_{\mathrm{clr}}(1 - C) + S_{\mathrm{cld}}C] + (T_{\mathrm{cld,real}} - T_{\mathrm{clr,real}})S_c + (\Delta_{\mathrm{cld}} - \Delta_{\mathrm{clr}})S_c. \quad (2)$$

In Eq. (1), the first component of S_{all} in brackets is the combination of the cloud-free surface temperature trend weighted by the cloud-free areal fraction and the cloudy surface temperature trend weighted by the cloud cover, which we call trend A hereinafter for convenience. The second term on the right represents the trend caused by cloud cover changes, which we call trend B. The surface temperature retrieval biases also have an effect on the all-sky trend, which is indicated as an expanded form of trend B in Eq. (2). This is a "false" trend that should be removed from the real trend.

Figure 3 shows the seasonal mean of the APP-x surface temperature difference under cloudy and cloud-free conditions. For most regions in the Arctic in winter, spring, autumn, and over the Arctic Ocean in summer the cloudy surface temperature is higher than

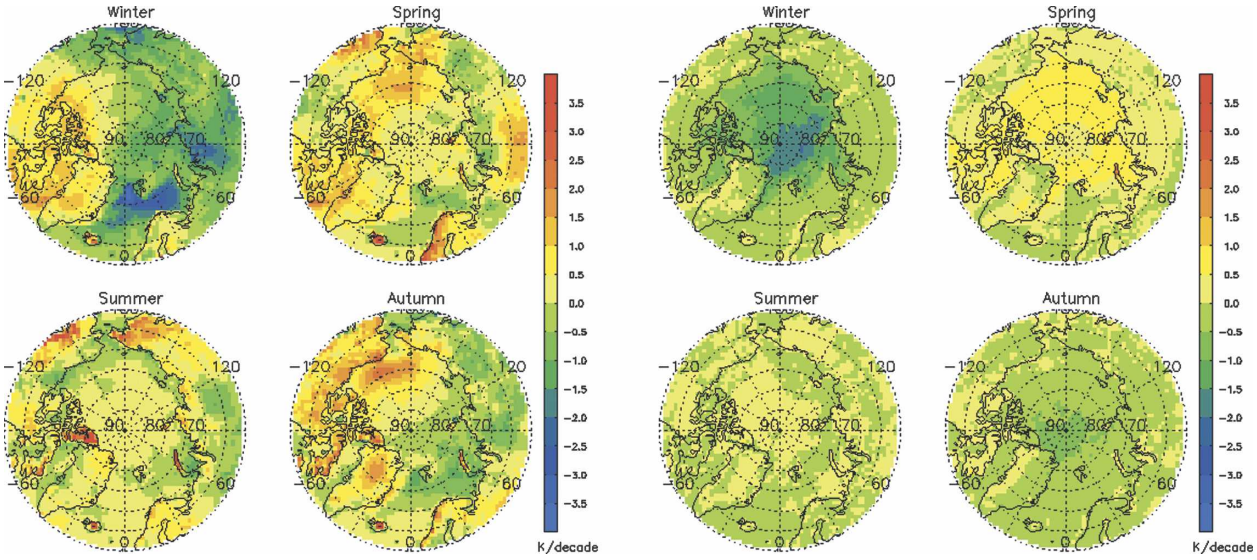

FIG. 4. The seasonal (left half) trend A and (right) trend B components of the total all-sky surface temperature trend from 1982 to 2004 based on the APP-x dataset.

that under cloud-free conditions because of the cloud radiative warming effect. The difference over the Arctic Ocean is around 8 K in winter and spring, 3 K in summer, and 6 K in autumn, which is consistent with the observed value over the Arctic Ocean reported by Walsh and Chapman (1998). Figure 1d shows the seasonal trend of APP-x cloud cover from 1982 to 2004. Over most regions in winter, the cloud cover decreases, especially over the Arctic Ocean in winter. Over most regions in spring, the cloud cover increases. In summer and autumn, the cloud cover does not change as significantly as in winter and spring. These trends are consistent with cloud cover trends reported by Schweiger (2004) based on TOVS Path-P dataset. These differences in surface temperature coupled with cloud cover trends produce the trend B portion of the total trend. According to Eq. (1), a negative trend B can be expected in winter and autumn, and a positive trend B can be expected in spring over the Arctic Ocean.

Figure 4 shows trend A (Fig. 4a) and trend B (Fig. 4b) based on the APP-x dataset from 1982 to 2004. Trend A is calculated as the first term in Eq. (1) using the data shown in Fig. 1a and 1b and seasonal mean cloud cover. Trend B is calculated as the second term in Eq. (1) using data shown in Figs. 3 and 1d. In winter, trend A has a similar pattern as the all-sky trend, which has an increasing trend in the western Arctic and a cooling trend over the eastern Arctic and most of the Arctic Ocean. Trend B is negative over most of the Arctic Ocean, with a magnitude from -0.4 to -1.5 K decade^{-1}. This trend arises from the higher surface temperature under cloudy conditions and the significant cloud cover decrease over the Arctic Ocean in winter. For regions over the Arctic Ocean with cooling total trends, trend B is -0.5 K decade^{-1} lower than trend A, which means that trend B contributes more than trend A to the total cooling over the eastern Arctic Ocean. The warming trend over the western Arctic Ocean could be higher if trend B were not decreasing.

In spring, trend A has a similar pattern to the all-sky trend, which shows warming over most regions in the Arctic; trend B is positive over the Arctic Ocean, with a magnitude around 0.5 K decade^{-1}. This trend originates from the higher surface temperature under cloudy conditions and increasing cloud cover over the Arctic Ocean in spring. Trend B is smaller over the Chukchi and Beaufort Seas and larger around the North Pole than that of the real trend, and the pattern of trend A dominates the all-sky trend pattern over land in the spring. In summer and autumn, trend B is smaller than in winter and spring, and trend A contributes most to the total trend. However, trend B around the North Pole in autumn is as high as -0.7 K decade^{-1}.

In addition to cloud cover changes and the difference between cloudy- and clear-sky surface temperatures, trend B is also a function of retrieval biases in the satellite-derived surface temperature. The relative importance of this trend in trend B depends on the ratio of the absolute magnitude of the difference between the clear- and cloudy-sky biases and the absolute magnitude of the real surface temperature difference under cloudy- and clear-sky conditions. For the sake of illustration, the cloudy- and clear-sky surface temperature

differences based on APP-x are 8, 8, 3, and 6 K, respectively, in winter, spring, summer, and autumn. If the bias difference is 2 K, the trend caused by bias difference will be 1/4, 1/4, 2/3, and 1/3 of trend B in winter, spring, summer, and autumn. This impact of retrieval biases is small but important. For example, in winter, the trend caused by the bias difference over the central Arctic will be -0.3 K decade^{-1}.

5. Discussion and conclusions

The all-sky surface temperature trends from 1982 to 2004 based on the APP-x dataset show warming trends over most regions in the Arctic spring and summer. In autumn, there is strong warming over the Beaufort Sea, the Chukchi Sea, Alaska, and northern Canada, though a cooling trend is evident over northern Russia. In winter, the cooling trend is significant over the eastern Arctic and most of the Arctic Ocean, with a warming trend over the western Arctic. A comparison of the all-sky surface temperature trends from APP-x and ERA-40 from 1982 to 2001 shows good agreement.

The surface temperature trends under cloud-free and cloudy conditions are spatially similar to the all-sky trends, indicating that the clear and cloudy trends are similar in sign. But the absolute magnitude of the trend under cloud-free conditions is larger than that under cloudy conditions.

A method was presented to separate the effect of changes in cloud cover from the total surface temperature trend. The surface temperature trend is partitioned into two parts: the first part (trend A) is the linear combination of the surface temperature trends under cloud-free and cloudy conditions; the second part (trend B) is caused by the trend in cloud cover and the surface temperature difference under cloudy- and clear-sky conditions. Trend B is significant in winter and spring over the Arctic Ocean because of the large cloud cover changes and cloudy–clear surface temperature differences. In winter, more than half of the decreasing surface temperature trend is from trend B over the central Arctic; that is, the trend in cloud cover significantly affects the trend in the all-sky surface temperature. In spring, trend A contributes more than trend B to the total trend over land and over the Chukchi and Beaufort Seas. In the autumn and summer, trend A dominates, because cloud cover trends are small and/or the clear–cloudy-sky temperature difference is small. The trend caused by a bias in the satellite retrieval of surface temperature is a part of trend B, and it accounts for 1/4, 1/4, 2/3, and 1/3 of trend B in winter, spring, summer, and autumn, respectively, given a retrieval bias difference of 2 K between cloudy- and clear-sky conditions.

In the process of partitioning the total surface temperature into trends A and B, the clear and cloudy surface temperature and cloud amount are assumed to change linearly over time. However, from Fig. 2, the total surface temperature shows low-frequency behavior, with variation of a few to 10 yr superimposed upon a general upward or downward trend. Similar patterns appear in APP-x cloud amount, clear and cloudy surface temperature, and the AO and sea ice extent. Long-term averages of cloud cover and the surface temperature difference under clear and cloudy conditions would minimize the nonlinear effect. The general trends of APP-x cloud amount and surface temperature are significant during the time period considered in this work. The basic conclusions presented above would be the same if the nonlinear effect were included.

The surface temperature trend will be nonzero if cloud cover changes significantly, even if the clear- and cloudy-sky surface temperatures remain constant. Significant total cloud cover changes are found in different regions of the globe, for example, 1.4% (of sky) per decade increasing total cloud cover in the United States since the late 1970s (Dai et al. 2006) and -0.88% per decade decreasing total cloud cover in China since the 1950s (Qian et al. 2006). The influence of cloud cover changes on the total surface temperature trend in the United States and China can be approximately -0.1 and 0.06 K decade^{-1}, respectively, under the assumption that the temperature difference under cloudy and clear conditions is -7 K in the midlatitudes. In the context of an observed 0.31 K decade^{-1} Northern Hemisphere land surface air temperature trend from 1976 to 2000 (Jones et al. 2001), this nonnegligible trend needs to be considered in studying regional surface temperature trends and their causes.

Acknowledgments. This research was supported by NSF Grants OPP-0240827 and OPP-0230317 and the NOAA SEARCH program. The APP product was provided by Chuck Fowler, Jim Maslanik, and the National Snow and Ice Data Center. The ERA-40 data were provided by ECMWF data services. The views, opinions, and findings contained in this report are those of the authors and should not be construed as an official National Oceanic and Atmospheric Administration or U.S. government position, policy, or decision.

REFERENCES

Cavalieri, D. J., C. L. Parkinson, and K. Y. Vinnikov, 2003: 30-year satellite record reveals contrasting Arctic and Antarctic decadal sea ice variability. *Geophys. Res. Lett.,* **30,** 1970, doi:10.1029/2003GL018031.

Chen, Y., J. A. Francis, and J. R. Miller, 2002: Surface temperature of the Arctic: Comparison of TOVS satellite retrievals with surface observations. *J. Climate,* **15,** 3698–3708.

Comiso, J. C., 2001: Satellite-observed variability and trend in sea-ice extent, surface temperature, albedo and clouds in the Arctic. *Ann. Glaciol.,* **33,** 457–473.

——, 2003: Warming trends in the Arctic from clear sky satellite observations. *J. Climate,* **16,** 3498–3510.

Curry, J. A., and E. E. Ebert, 1992: Annual cycle of radiation fluxes over the Arctic Ocean: Sensitivity to cloud optical properties. *J. Climate,* **5,** 1267–1280.

——, ——, and J. L. Schramm, 1993: Impact of clouds on the surface radiation balance of the Arctic Ocean. *Meteor. Atmos. Phys.,* **51,** 197–217.

——, W. B. Rossow, D. Randall, and J. L. Schramm, 1996: Overview of Arctic cloud and radiation characteristics. *J. Climate,* **9,** 1731–1764.

Dai, A., T. R. Karl, B. Sun, and K. E. Trenberth, 2006: Recent trends in cloudiness over the United States: A tale of monitoring inadequacies. *Bull. Amer. Meteor. Soc.,* **87,** 597–606.

Dong, X., and G. G. Mace, 2003: Arctic stratus cloud properties and radiative forcing derived from ground-based data collected at Barrow, Alaska. *J. Climate,* **16,** 445–461.

Groves, D. G., and J. A. Francis, 2002: Variability of the Arctic atmospheric moisture budget from TOVS satellite data. *J. Geophys. Res.,* **107D,** 4785, doi:10.1029/2002JD002285.

Houghton, J. T., Y. Ding, D. J. Griggs, M. Noguer, P. J. van der Linden, X. Dai, K. Maskell, and C. A. Johnson, Eds, 2001: *Climate Change 2001: The Scientific Basis.* Cambridge University Press, 881 pp.

Intrieri, J. M., C. W. Fairall, M. D. Shupe, P. O. G. Persson, E. L. Andreas, P. S. Guest, and R. E. Moritz, 2002: An annual cycle of Arctic surface cloud forcing at SHEBA. *J. Geophys. Res.,* **107C,** 8039, doi:10.1029/2000JC000439.

Jones, P. D., T. J. Osborn, K. R. Briffa, C. K. Folland, E. B. Horton, L. V. Alexander, D. E. Parker, and N. A. Rayner, 2001: Adjusting for sampling density in grid box land and ocean surface temperature time series. *J. Geophys. Res.,* **106D,** 3371–3380.

Key, J. R., 2002: The cloud and surface parameter retrieval (CASPR) system for polar AVHRR. Cooperative Institute for Meteorological Satellite Studies, University of Wisconsin—Madison, 69 pp. [Available online at stratus.ssec.wisc.edu/caspr/documentation.html.]

——, and R. G. Barry, 1989: Cloud cover analysis with Arctic AVHRR data. 1. Cloud detection. *J. Geophys. Res.,* **94D,** 18 521–18 535.

——, and M. Haefliger, 1992: Arctic ice surface temperature retrieval from AVHRR thermal channels. *J. Geophys. Res.,* **97D,** 5885–5893.

——, and A. M. Wong, 1999: Estimating the cloudy sky surface temperature of sea ice with optical satellite data. *Proc. IGARSS'99,* Hamburg, Germany, IEEE, 320–322.

——, and J. M. Intrieri, 2000: Cloud particle phase determination with the AVHRR. *J. Appl. Meteor.,* **39,** 1797–1804.

——, J. B. Collins, C. Fowler, and R. S. Stone, 1997: High-latitude surface temperature estimates from thermal satellite data. *Remote Sens. Environ.,* **61,** 302–309.

——, D. Slayback, C. Xu, and A. Schweiger, 1999: New climatologies of polar clouds and radiation based on the ISCCP "D" products. Preprints*, Fifth Conf. on Polar Meteorology and Oceanography,* Dallas, TX, Amer. Meteor. Soc., 227–232.

——, X. Wang, J. C. Stoeve, and C. Fowler, 2001: Estimating the cloudy-sky albedo of sea ice and snow from space. *J. Geophys. Res.,* **106D,** 12 489–12 498.

King, M. D., S. Platnick, P. Yang, G. T. Arnold, M. A. Gray, J. C. Riedi, S. A. Ackerman, and K.-N. Liou, 2004: Remote sensing of liquid water and ice cloud optical thickness and effective radius in the Arctic: Application of airborne multispectral MAS data. *J. Atmos. Oceanic Technol.,* **21,** 857–875.

Liu, J. P., J. A. Curry, and Y. Y. Hu, 2004: Recent Arctic sea ice variability: Connections to the Arctic Oscillation and the ENSO. *Geophys. Res. Lett.,* **31,** L09211, doi:10.1029/2004GL019858.

Manabe, S., M. J. Spelman, and R. J. Stouffer, 1992: Transient responses of a coupled ocean–atmosphere model to gradual changes of atmospheric CO_2. Part II: Seasonal response. *J. Climate,* **5,** 105–126.

Maslanik, J. A., J. Key, C. W. Fowler, T. Nguyen, and X. Wang, 2001: Spatial and temporal variability of satellite-derived cloud and surface characteristics during FIRE-ACE. *J. Geophys. Res.,* **106D,** 15 233–15 250.

McPhee, M. G., T. P. Stanton, J. H. Morison, and D. G. Martinson, 1998: Freshening of the upper ocean in the Arctic: Is perennial sea ice disappearing? *Geophys. Res. Lett.,* **25,** 1729–1732.

Meier, W., J. A. Maslanik, J. R. Key, and C. W. Fowler, 1997: Multiparameter AVHRR-derived products for Arctic climate studies. *Earth Interactions,* **1.** [Available online at http://EarthInteractions.org.]

Parkinson, C. L., and D. J. Cavalieri, 2002: A 21 year record of Arctic sea-ice extents and their regional, seasonal, and monthly variability and trends. *Ann. Glaciol.,* **34,** 441–446.

——, ——, P. Gloersen, H. J. Zwally, and J. C. Comiso, 1999: Arctic sea ice extents, areas, and trends, 1978–1996. *J. Geophys. Res.,* **104C,** 20 837–20 856.

Qian, Y., D. P. Kaiser, L. R. Leung, and M. Xu, 2006: More frequent cloud-free sky and less surface solar radiation in China from 1955 to 2000. *Geophys. Res. Lett.,* **33,** L01812, doi:10.1029/2005GL024586.

Randall, D., and Coauthors, 1998: Status of and outlook for large-scale modeling of atmosphere–ice–ocean interactions in the Arctic. *Bull. Amer. Meteor. Soc.,* **79,** 197–219.

Rigor, I. G., R. L. Colony, and S. Martin, 2000: Variations in surface air temperature observations in the Arctic, 1979–97. *J. Climate,* **13,** 896–914.

——, ——, and J. M. Wallace, 2002: Response of sea ice to the Arctic Oscillation. *J. Climate,* **15,** 2648–2663.

Schweiger, A. J., 2004: Changes in seasonal cloud cover over the Arctic seas from satellite and surface observations. *Geophys. Res. Lett.,* **31,** L12207, doi:10.1029/2004GL020067.

——, and J. R. Key, 1994: Arctic Ocean radiative fluxes and cloud forcing estimated from the ISCCP C2 cloud dataset, 1983–1990. *J. Appl. Meteor.,* **33,** 948–963.

Serreze, M. C., and Coauthors, 2000: Observational evidence of recent change in the northern high-latitude environment. *Climatic Change,* **46,** 159–207.

Shupe, M. D., and J. M. Intrieri, 2004: Cloud radiative forcing of the Arctic surface: The influence of cloud properties, surface albedo, and solar zenith angle. *J. Climate,* **17,** 616–628.

Stroeve, J. C., J. E. Box, C. Fowler, T. Haran, and J. Key, 2001: Intercomparison between in situ and AVHRR Polar Pathfinder-derived surface albedo over Greenland. *Remote Sens. Environ.,* **75,** 360–374.

Thompson, D. W. J., and J. M. Wallace, 1998: The Arctic Oscillation signature in the wintertime geopotential height and temperature fields. *Geophys. Res. Lett.,* **25,** 1297–1300.

——, ——, and G. C. Hegerl, 2000: Annular modes in the extratropical circulation. Part II: Trends. *J. Climate,* **13,** 1018–1036.

Uppala, S. M., and Coauthors, 2005: The ERA-40 re-analysis. *Quart. J. Roy. Meteor. Soc.,* **131,** 2961–3012.

Uttal, T., and Coauthors, 2002: Surface heat budget of the Arctic Ocean. *Bull. Amer. Meteor. Soc.,* **83,** 255–275.

Walsh, J. E., and W. L. Chapman, 1998: Arctic cloud–radiation–temperature associations in observational data and atmospheric reanalyses. *J. Climate,* **11,** 3030–3045.

Wang, X., and J. R. Key, 2003: Recent trends in Arctic surface, cloud, and radiation properties from space. *Science,* **299,** 1725–1728.

——, and ——, 2005a: Arctic surface, cloud, and radiation properties based on the AVHRR Polar Pathfinder dataset. Part I: Spatial and temporal characteristics. *J. Climate,* **18,** 2558–2574.

——, and ——, 2005b: Arctic surface, cloud, and radiation properties based on the AVHRR Polar Pathfinder dataset. Part II: Recent trends. *J. Climate,* **18,** 2575–2593.